

Revealing silicon crystal defects by conductive atomic force microscope

Liu, Xiaoxiao; Yu, Bingjun; Zou, Yijia; Zhou, Chao; Li, Xiaoying; Wu, Jiang; Liu, Huiyun; Chen, Lei; Qian, Linmao

DOI:

[10.1063/1.5044518](https://doi.org/10.1063/1.5044518)

License:

Other (please specify with Rights Statement)

Document Version

Peer reviewed version

Citation for published version (Harvard):

Liu, X, Yu, B, Zou, Y, Zhou, C, Li, X, Wu, J, Liu, H, Chen, L & Qian, L 2018, 'Revealing silicon crystal defects by conductive atomic force microscope', *Applied Physics Letters*, vol. 113, no. 10, 101601.
<https://doi.org/10.1063/1.5044518>

[Link to publication on Research at Birmingham portal](#)

Publisher Rights Statement:

Checked for eligibility: 13/11/2018

This article may be downloaded for personal use only. Any other use requires prior permission of the author and AIP Publishing. The following article appeared in Liu, X., Yu, B., Zou, Y., Zhou, C., Li, X., Wu, J., Liu, H., Chen, L. and Qian, L., 2018. Revealing silicon crystal defects by conductive atomic force microscope. *Applied Physics Letters*, 113(10), p.101601. and may be found at: <https://doi.org/10.1063/1.5044518>

General rights

Unless a licence is specified above, all rights (including copyright and moral rights) in this document are retained by the authors and/or the copyright holders. The express permission of the copyright holder must be obtained for any use of this material other than for purposes permitted by law.

- Users may freely distribute the URL that is used to identify this publication.
- Users may download and/or print one copy of the publication from the University of Birmingham research portal for the purpose of private study or non-commercial research.
- User may use extracts from the document in line with the concept of 'fair dealing' under the Copyright, Designs and Patents Act 1988 (?)
- Users may not further distribute the material nor use it for the purposes of commercial gain.

Where a licence is displayed above, please note the terms and conditions of the licence govern your use of this document.

When citing, please reference the published version.

Take down policy

While the University of Birmingham exercises care and attention in making items available there are rare occasions when an item has been uploaded in error or has been deemed to be commercially or otherwise sensitive.

If you believe that this is the case for this document, please contact UBIRA@lists.bham.ac.uk providing details and we will remove access to the work immediately and investigate.

Revealing silicon crystal defects by conductive atomic force microscope

Xiaoxiao Liu,¹ Bingjun Yu,^{1,a)} Yijia Zou,¹ Chao Zhou,¹ Xiaoying Li,² Jiang Wu,³ Huiyun Liu,³
Lei Chen,¹ Linmao Qian¹

¹ *Tribology Research Institute, Key Laboratory of Advanced Technologies of Materials (Ministry of Education), Southwest Jiaotong University, Chengdu 610031, Sichuan Province, P. R. China*

² *School of Metallurgy and Materials, The University of Birmingham, Birmingham B15 2TT, UK*

³ *Department of Electronic & Electrical Engineering, University College London, Torrington Place, London WC1E 7JE, UK*

^{a)} *E-mail address: bingjun@swjtu.edu.cn; Tel.: +86 28 87634181; Fax: +86 28 87603142*

Abstract

The machining and polishing of silicon can damage its surface. Therefore, the investigation of electric performance of processed surface is of paramount importance for understanding and improving the utilization of silicon components with nanoscale crystal defects. In this study, conductivity of nanoscratches on silicon surface was investigated by conductive atomic force microscope. Compared to original silicon surface (without any treatment), electrical breakover at low bias voltage could be detected on mechanically scratched area of silicon surface with crystal defects, and the current increased with the voltage. In contrast, no obvious current was found on defect-free scratch created by tribochemical removal. The conductivity could also be observed on a friction-induced protrusive hillock created at high speed, but not on a hillock created at low speed that is constructed by amorphous silicon. Further analysis showed that lattice distortions could facilitate easy electron flow and contributed significantly to the conductivity of a mechanical scratch on silicon surface; however, amorphous layer hardly contributed to the conductivity, which was also supported by high resolution transmission electron microscope analysis. As a result, the relation between the electrical performance and microstructures was experimentally established. These findings shed new light on subtle mechanism of defect-dependent conductivity, and also provide a rapid and nondestructive method for detecting surface defects.

Monocrystalline silicon (Si) presents excellent electrical and mechanical properties, and services as a fundamental semiconductor material in modern technological applications, such as integrated circuits (IC), micro/nanomechanical systems (MEMS/NEMES), photovoltaic devices, and so on.^{1,2} It is of great importance to obtain silicon wafers with smooth surface by material removing processes such as machining, cutting and milling from nanoscale to macroscale.³⁻⁵ However, the manufacturing can usually result in the destructions of silicon surface and subsurface.^{6,7} Such damage significantly influences the mechanical and electrical properties of silicon, and can even degrade the performance of devices engineered using it.⁸

In the past years, extensive research efforts have been focused on revealing the deformation mechanism of materials or controlling damages during scratch and indentation tests;^{9 - 12} however, limited research has been devoted to the detection of electronical performances of damaged silicon surface or structures that play unexpected role in affecting the properties of component employed. It has been proven that several types of silicon crystals, such as amorphous silicon (a-Si), Si-II (β -Sn), and Si-XII/Si-III (or R8/BC8) phases, can be created by the indentation, and the critical pressures for the formation of these phases can be predicted accurately by simulations.¹²⁻¹⁴ Some phases were also detected after scratching.^{15,16} These crystal defects can lead to the change in physical and chemical performance, such as transmission of infrared light and selective etching in alkali-based solutions.¹⁷⁻¹⁹ The change in the conductivity was also detected on the indented area on Si(100) surface, and it was speculated that high current sites corresponded directly to Si-III and/or Si-XII phases toward the indent edge.^{20,21}

Owing to the combination of shear and stress in scratching, significant difference is noticed in damage formation between the indentation and scratch tests. For example, low applied contact pressure can hardly lead to the plastic deformation of silicon during indentation, but can cause obvious surface damage or crystal deformation during scratching.¹⁶ Owing to the mixed chemical and physical interactions at the sliding interface, multiple silicon crystals can be produced by scratching,^{15,16,22} and it remains difficult to differentiate among the contribution of some crystal phases, such as amorphous layer and other crystal distortions, toward the conductivity change on silicon surface. Although the formation of amorphous silicon structure is suggested to be a main contributor to the conductivity increase of a mechanical scratch on silicon surface at a given bias voltage,²³ detailed analysis is still required to support the state. By far, the relation between the electrical performance and microstructures has not been experimentally established, and further study toward revealing the mechanistic approach for the nanoscratching-induced conductivity change of silicon still lacks and highly desirable. On

the other hand, the detection of surface/subsurface defects at nanoscale is significantly important for understanding and improving the utilization of silicon components with crystal defects. Although high resolution transmission electron microscope (HRTEM) shows robust ability in observing crystal lattice on the cross section of processed surface, it depends on focused ion beam (FIB) milling of specimen surface and thus causes destruction of the surface.¹⁶ Chemical etching can usually result in local damages of processed area, and the etching agent can cause surface pollution. Therefore, a rapid, cost effective, and nondestructive method is highly desirable for detecting damages at nanoscale on monocrystalline silicon.

In the present study, the electrical breakover of a surface scratch on silicon was investigated by conductive atomic force microscope (CAFM). For comparison, the conductivity of defect-free structures and friction-induced protrusive hillocks was also detected. The mechanism for the breakover on mechanically scratched area was further proposed based on HRTEM study. Finally, the application of conductivity characterization was also demonstrated in detecting surface damage of silicon.

B-doped Si(100) wafers (MEMC Electronic Materials, Inc., USA) with a resistivity of 10 Ω -cm were used for scratch production and conductivity test using an atomic force microscope (AFM; E-Sweep, Hitachi Instruments Inc., Japan). The surface root-mean-square (RMS) roughness of the silicon wafers was measured to be about 0.1 nm over the area of 1 $\mu\text{m} \times 1 \mu\text{m}$ by AFM. The samples were ultrasonically cleaned with acetone, ethanol, and deionized water successively for 3 min to remove surface contaminations. A home-built micro/nano-scratching device was employed for producing mechanical scratches on silicon surface under temperature of $\sim 25^\circ\text{C}$ and relative humidity of $\sim 55\%$. A conical diamond tip with the tip radius R of about 10 μm was used for scratching under normal load F_n ranging from 5 to 20 mN. A PtIr-coated conductive AFM probe (SCM-PIC, Bruker Corporation, USA) with the nominal tip radius R of 20 nm was used to characterize sample conductivity in vacuum (~ 1 Pa) by conductive AFM (CAFM). For comparison, CAFM tests were also performed on protrusive hillocks produced using a diamond tip ($R = 0.5 \mu\text{m}$) under different sliding velocities (10-1000 $\mu\text{m/s}$) and on defect-free grooves produced using a SiO_2 tip ($R = 1 \mu\text{m}$). To prevent the generation of displacement current resulting from high scanning speed, the scanning speed of 0.6 $\mu\text{m/s}$ was set as the optimized speed in the present study for conductivity detection.²⁴ Negative bias voltage of -0.5 V to -3.0 V was applied to the scratch to avoid the anodic oxidation of the scanned area on silicon surface.

The surface topography and current image of the scratch produced under different loads

from 5 to 20 mN are shown in Fig. 1(a). The cross-section profiles of the topography exhibit that the depth of the V-shaped scratch increases from 15 to 250 nm with applied loads. The current images indicate that obvious electrical breakover signals are detected on the scratches; however, no conductivity is observed on the original silicon surface under the given test. No obvious changes in the corresponding maximum current are found under different scratching depth at the same voltage of -2.0 V (Fig. 1(b)). Nonetheless, the increase in the bias voltage from -0.5 V to -3.0 V can lead to obvious increase of the current from the same scratch (Fig. 1(c)). Moreover, the discontinuity of current was detected on the scratch, in particular, for the one produced under high load, which may be ascribed to the different types of deformation beneath the scratch. It is noteworthy that micro cracks can facilitate the breakover on silicon surface. Under the applied load of 20 mN, obvious current signal was detected on the cracks besides the scratch as marked by arrows in Figs. 1(a) and (b).

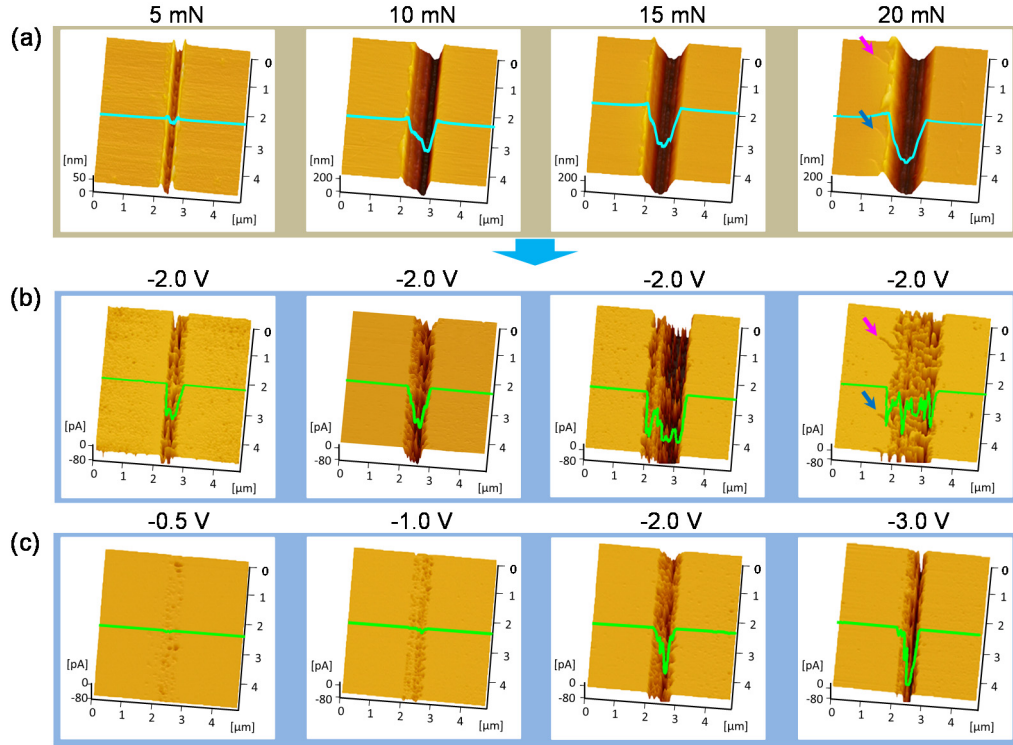


FIG. 1. Conductivity detection of nanoscratches on silicon surface in vacuum: (a) Topographies and (b) corresponding current images of scratches created under different normal loads (5, 10, 15 and 20 mN). For obtaining the current images in (b), the applied bias voltage is -2.0 V. (c) Current images of the scratch created under 10 mN, and the voltage is -0.5, -1.0, -2.0 and -3.0 V, respectively. The corresponding cross-section profiles were obtained from the AFM topographies or current images, and shown in the figures with the same scale.

By friction-induced tribochemical removal or tribochemistry-induced selective etching, defect-free grooves can be produced on silicon surface, without any crystal defects underneath the removed area.^{17,25} The defect-free scratch with the depth of ~ 3 nm was fabricated on Si(100) surface using a SiO₂ tip by tribochemical removal, and a groove of ~ 60 nm was also prepared by tribochemistry-induced selective etching, as shown in Fig. 2(a). After characterization by CAFM, hardly any difference in conductivity could be observed between the scratch and the original silicon surface under the bias voltage of -2.0 V, as shown in Fig. 2(b). Therefore, combining CAFM investigations on the mechanical and defect-free scratches revealed that the subsurface damage induced by scratching could result in local conductivity on the scratch.

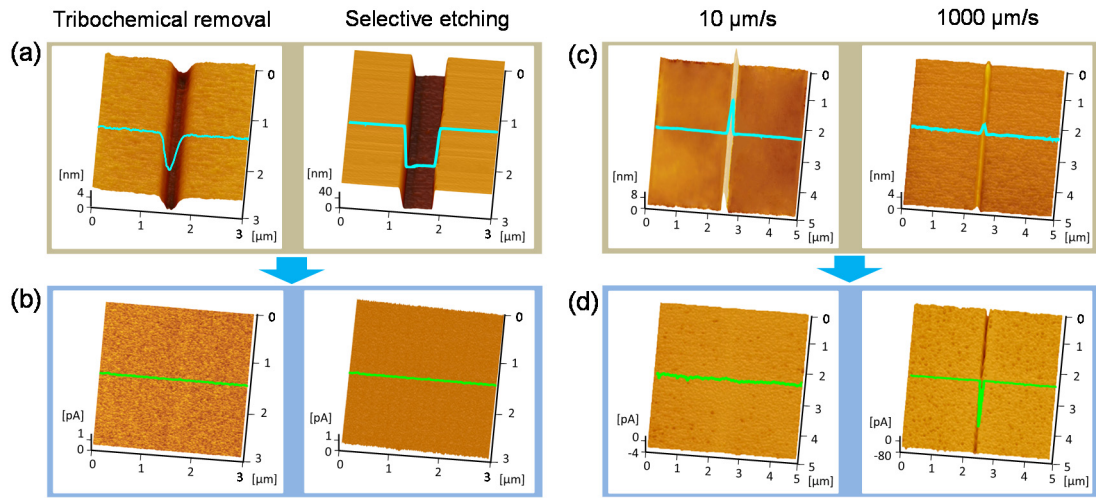


FIG. 2. Conductivity detection of (a,b) defect-free grooves and (c,d) protrusive hillocks on silicon. (a) Topographies of defect-free grooves created by tribochemical removal using a SiO₂ tip and by tribochemistry-induced selective etching. (c) Topographies of friction-induced protrusive hillocks produced under sliding speed of 10 $\mu\text{m/s}$ and 1000 $\mu\text{m/s}$, respectively. (b) and (d) show the corresponding current images detected from the above mentioned grooves, and the bias voltage for conductivity detection is -2.0 V. The corresponding cross-section profiles are also shown in the images.

For further comparison, some protrusive hillocks were produced on silicon surface by scratching using a diamond tip under the Hertz contact pressure estimated lower than the hardness of silicon (~ 11 GPa).^{16,22} In the present study, different protrusive hillocks were produced on silicon under different sliding speeds and then detected by CAFM (Fig. 2). The results indicated that the conductivity measured from the hillock on silicon increased with the sliding speed for the hillock production.¹⁶ Under the sliding speed of 10 $\mu\text{m/s}$, although the

hillock was the highest in this study, hardly any conductivity could be detected as shown in Figs. 2(c) and 2(d).. In contrast, obvious conductivity was observed on the hillock produced at 1000 $\mu\text{m/s}$ although its height was ~ 1 nm (Fig. 2c).

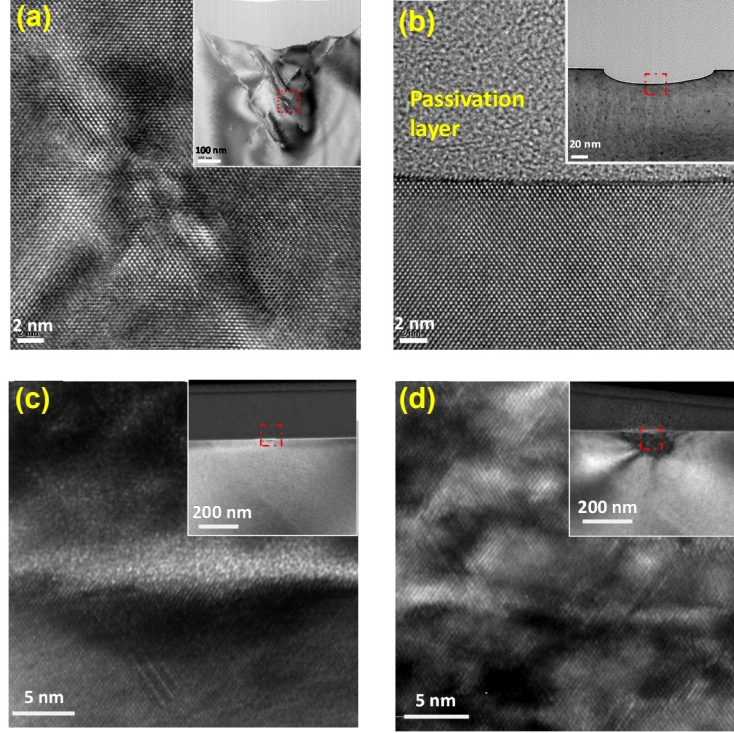


FIG. 3. TEM detection of the cross sections of different scratches and hillocks on silicon surface: (a) Mechanical scratch created using a diamond tip under an applied load F_n of 20 mN in air, (b) A defect-free scratch created using a SiO_2 tip ($R = 1 \mu\text{m}$) under reciprocating scratching cycles of 100 and $F_n = 3 \mu\text{N}$, (c) A protrusive hillock created using a diamond tip at 10 $\mu\text{m/s}$, and (d) A protrusive hillock created using a diamond tip at 1000 $\mu\text{m/s}$. The marked area by dotted frame in the inset was magnified below for every image.

Fig. 3 shows HRTEM characterization of the cross sections of different scratches and hillocks on silicon surface. Severe lattice sliding and mixed lattice distortions were observed on the cross section of the groove generated by mechanical removal (Fig. 3(a)); however, no obvious lattice defect could be found on the groove created using a SiO_2 tip through tribochemical removal (Fig. 3(b)). For the hillock produced under low slinging speed (10 $\mu\text{m/s}$), amorphous silicon with slight stacking faults constituted the main composition (Fig. 3(c)). In contrast, intensive dislocations, stacking faults, and slip lines were found below the hillock produced under high slinging speed (1000 $\mu\text{m/s}$). Combined results of the conductive tests of the mechanical scratches, defect-free grooves, and protrusive hillocks constructed by

amorphous or severe distortions indicate that the friction-induced amorphous layer has no contribution to the conductivity of silicon scratch; however, crystal distortions contribute significantly to the conductivity of the mechanical scratch.

As a result, the mechanism of electrical breakover in the mechanical scratch can be ascribed to the formation of new lattice structures beneath. It has been reported that some phases can lead to a narrow band gap compared to doped monocrystalline silicon. For example, Si-IV behaves like a semiconductor with an intermediate (~ 1 eV) band gap.²⁶ Based on the present results, it can be hereby speculated that the existence of dislocations, stacking faults, and slip lines easily facilitate the electron flow compared to bulk silicon and amorphous silicon. Moreover, it was also deduced that the residual stress existing in the deformed part could reduce the critical energy for carrier transportation, which could facilitate more carriers passing through the stressed area.^{27,28} Therefore, when the AFM tip scans on the bulk silicon surface, few electrons can get through the crystal region due to the limited electron holes in the doped silicon at low bias voltage, as shown in Fig. 4(a). In contrast, the lattice distortions are expected to provide a low circulation barrier for electron pass, and the electricity can circulate through it easily when the tip scans on the groove with crystal distortions (Fig. 4(b)). In addition, crystal distortions and micro cracks can result in unsaturated bonds with respect to the bulk structure, and the unsaturated bonds are speculated to be the channels for promoting electron flow. However, some theoretical simulations maybe still required for further revealing the nature of the electrical breakover in the mechanical scratch with crystal damages.

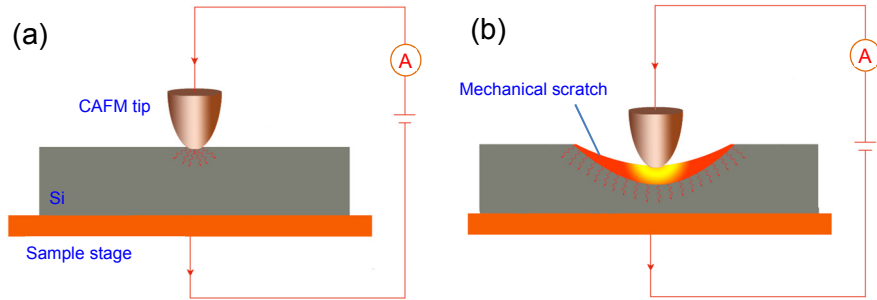


FIG. 4. The schematic illustration of the conductivity of (a) bulk silicon and (b) a scratch on silicon.

The change in the conductivity can be applied for detecting defects on silicon surface as well as gallium arsenide (GaAs) surface. Fig. 5(a) demonstrates that when Si(100) surface was polished with the slurry containing SiC particles, some scratches were formed. Obvious current signal could be observed for the mechanical scratches, indicating severe lattice damages

beneath (Fig. 5(b)). Mechanical scratches on other silicon planes, such as Si(110) and Si(111), and GaAs wafer could also be differentiated by CAFM. It was highlighted that micro cracks could facilitate the conductivity of silicon surface, as shown in Figs. 1(a) and (b). Such a method can help monitor and optimize the surface quality of silicon during its manufacturing processes. Moreover, the present study may shed new light on understanding the electrical performance of silicon components with crystal defects as well as micro/nano-cracks, and it seems that amorphization should be avoided in silicon processing. However, it is still difficult to differentiate a given silicon phase, such as Si-II, Si-III, or Si-XII/Si-XIII, because the formation of each one of these phases can be hardly controlled accurately by indentations or scratch at the present stage.

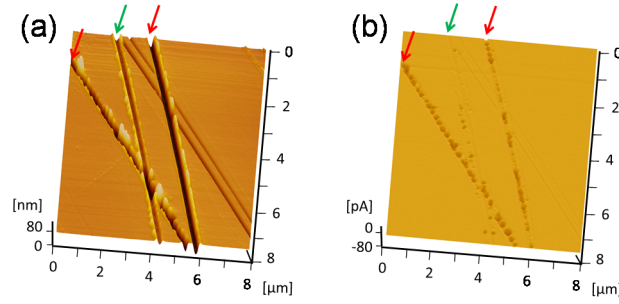


FIG. 5. Detection of surface defects on silicon after being polished with the slurry containing SiC particles: (a) AFM topography and (b) the corresponding current image.

In this study, electrical breakover was observed on a mechanical scratch on monocrystalline silicon at low bias voltage by CAFM. Comparative analysis indicated that the change in conductivity could not be found on a friction-induced hillock with amorphous structure or on a defect-free scratch. It was also deduced that lattice distortions including dislocations, stacking faults, and slips easily facilitated the electron flow compared to bulk silicon and amorphous silicon, and contributed significantly to the conductivity of a mechanical scratch on silicon. The proposed study provides alternative approach for rapid and nondestructive detection of crystal damages on silicon, and sheds new light on understanding the electrical performance of silicon components with crystal defects as well as micro/nano-cracks.

This work was supported by the National Natural Science Foundation of China (Grant No. 51775462).

- ¹S. H. Baek, J. Park, D. M. Kim, V. A. Aksyuk, R. R. Das, S. D. Bu, D. A. Felker, J. Lettieri, V. Vaithyanathan, S. S. Bharadwaja, N. Bassiri-Gharb, Y. B. Chen, H. P. Sun, C. M. Folkman, H. W. Jang, D. J. Kreft, S. K. Streiffer, R. Ramesh, X. Q. Pan, S. Trolrier-McKinstry, D. G. Schlom, M. S. Rzechowski, R. H. Blick, and C. B. Eom, *Science* **334**(6058), 958 (2011).
- ²F. Priolo, T. Gregorkiewicz, M. Galli, and T. F. Krauss, *Nat. Nanotech.* **9**(1), 19 (2014).
- ³B. J. Yu, H. T. He, L. Chen, and L. M. Qian, *Wear* **374-375**, 29 (2017).
- ⁴J. Yan, T. Asami, H. Harada, and T. Kuriyagawa, *CIRP Ann. Manuf. Technol.* **61**(1), 131 (2012).
- ⁵F. Z. Fang, Y. H. Chen, X. D. Zhang, X. T. Hu, and G. X. Zhang, *CIRP Ann.-Manuf. Techn.* **60**(1), 527 (2011).
- ⁶Y. Yang, K. DeMunck, R. C. Teixeira, B. Swinnen, B. Verlinden, and I. DeWolf, *Semicond Sci. Tech.* **23**(7), 075038 (2008).
- ⁷J. Yan, T. Asami, H. Harada, and T. Kuriyagawa, *Precis. Eng.* **33**(4), 378 (2009).
- ⁸H. Liu, T. Wang, Q. Jiang, R. Hogg, F. Tutu, and A. Seeds, *Nat. Photon.* **5** (7), 416 (2011).
- ⁹Y. Gogotsi, G. Zhou, S. S. Ku, and S. Cetinkunt, *Semicond. Sci. Tech.* **16**(5), 345 (2001).
- ¹⁰S. Z. Chavoshi, S. C. Gallo, H. Dong, and X. Luo, *Mat. Sci. Eng. A* **684**, 385 (2017).
- ¹¹S. Goel, N. Haque Faisal, X. Luo, J. Yan, and A. Agrawal, *J. Phys. D Appl. Phys.* **47**(27), 275304 (2014).
- ¹²J. I. Jang, M. J. Lance, S. Wen, T. Y. Tsui, and G. M. Pharr, *Acta Mater.* **53**, 1759 (2005).
- ¹³K. Mylvaganam, L. C. Zhang, P. Eyben, J. Mody, and W. Vandervorst, *Nanotechnology* **20**, 305705 (2009).
- ¹⁴I. Zarudi, J. Zou, and L. C. Zhang, *Appl. Phys. Lett.* **82**(6), 874 (2003).
- ¹⁵Y. Q. Wu, H. Huang, J. Zou, L. C. Zhang, and J. M. Dell, *Scripta Mater.* **63**(8), 847 (2010).
- ¹⁶B. J. Yu, X. Y. Li, H. S. Dong, Y. F. Chen, L. M. Qian, and Z. R. Zhou, *J. Phys. D Appl. Phys.* **45**, 145301 (2012).
- ¹⁷J. Guo, B. J. Yu, L. Chen, and L. M. Qian, *Sci. Rep.* **5**, 16472 (2015).
- ¹⁸C. N. Jin, B. J. Yu, C. Xiao, L. Chen, and L. M. Qian, *Nanoscale Res. Lett.* **11**, 229 (2016).
- ¹⁹L. Dong, J. A. Patten, and J. A. Miller, *Int. J. Manufacturing Technology and Management* **7**(5-6), 530 (2005).
- ²⁰S. T. Ho, Y. H. Chang, and H. N. Lin, *J. Appl. Phys.* **96**(6), 3562 (2004).
- ²¹S. Ruffell, J.E. Bradby, J.S. Williams, and O.L. Warren, *J. Mater. Res.* **22**(3), 578 (2007).
- ²²B. J. Yu, H. S. Dong, L. M. Qian, Y. F. Chen, J. X. Yu, and Z. R. Zhou, *Nanotechnology* **20**, 465303 (2009).
- ²³O. G. Lysenko, S. N. Dub, V. I. Grushko, E. I. Mitskevich, and G. N. Tolmacheva, *J. Superhard Mater.* **35**(6), 350 (2013).
- ²⁴Z. L. Wang, *Mater. Today* **20**(2), 74 (2017).
- ²⁵L. Chen, J. L. Wen, P. Zhang, B. J. Yu, T. B. Ma, X.C Lu, S. H. Kim, and L. M. Qian, *Nat. Commun.* **9**, 1542 (2018).
- ²⁶J. M. Besson, E. H. Mokhtari, J. Gonzalez, and G. Weil, *Phys. Rev. Lett.* **59**(4), 473 (1987).
- ²⁷M. V. Fischetti, and S. E. Laux, *J. Appl. Phys.* **80**(4), 2234 (1996).

²⁸S.Mayuzumi, S. Yamakawa, D. Kosemura, M. Takei, K. Nagata, H. Akamatsu, H. Wakabayashi, K. Amari, Y. Tateshita, M. Tsukamoto, T. Ohno, A. Ogura, and N. Nagashima, IEEE T. Electron Dev. **57(6)**, 1295 (2010).